

Ultrasensitive Quantification of Tumor mRNAs in Extracellular Vesicles with Integrated Microfluidic Digital Analysis Chip

Peng Zhang¹, Jennifer Crow², Divya Lella¹, Xin Zhou¹, Glenson Samuel^{3,4}, Andrew K. Godwin^{2,4*}, and Yong Zeng^{1,4*}

¹Department of Chemistry and Bioengineering Graduate Program, University of Kansas, Lawrence, KS USA

²Department of Pathology and Laboratory Medicine, University of Kansas Medical Center, Kansas City, KS, USA

³Division of Hematology, Oncology and Bone Marrow Transplant, Children's Mercy Hospitals & Clinics, Kansas City, KS, USA

⁴University of Kansas Cancer Center, Kansas City, KS, USA

*Corresponding Authors:

Yong Zeng, E-mail: yongz@ku.edu, Fax: +1 785 864 5396

Andrew K., Godwin, E-mail: agodwin@kumc.edu, Fax: +1 913 945 6327

SUPPORTING INFORMATION

Table of Contents:

1. Figure S1	S-2
2. Figure S2	S-3
3. Figure S3	S-4
4. Figure S4	S-4
5. Figure S5	S-5
6. Table S1. Probability calculation	S-5
7. Table S2. Sequences of probes	S-6
8. Table S3. Synthetic <i>GAPDH</i> mRNA.....	S-6
9. Table S4. PNET Fusion and breakpoints	S-7
10. Table S5. Characterization of isolated EVs	S-7

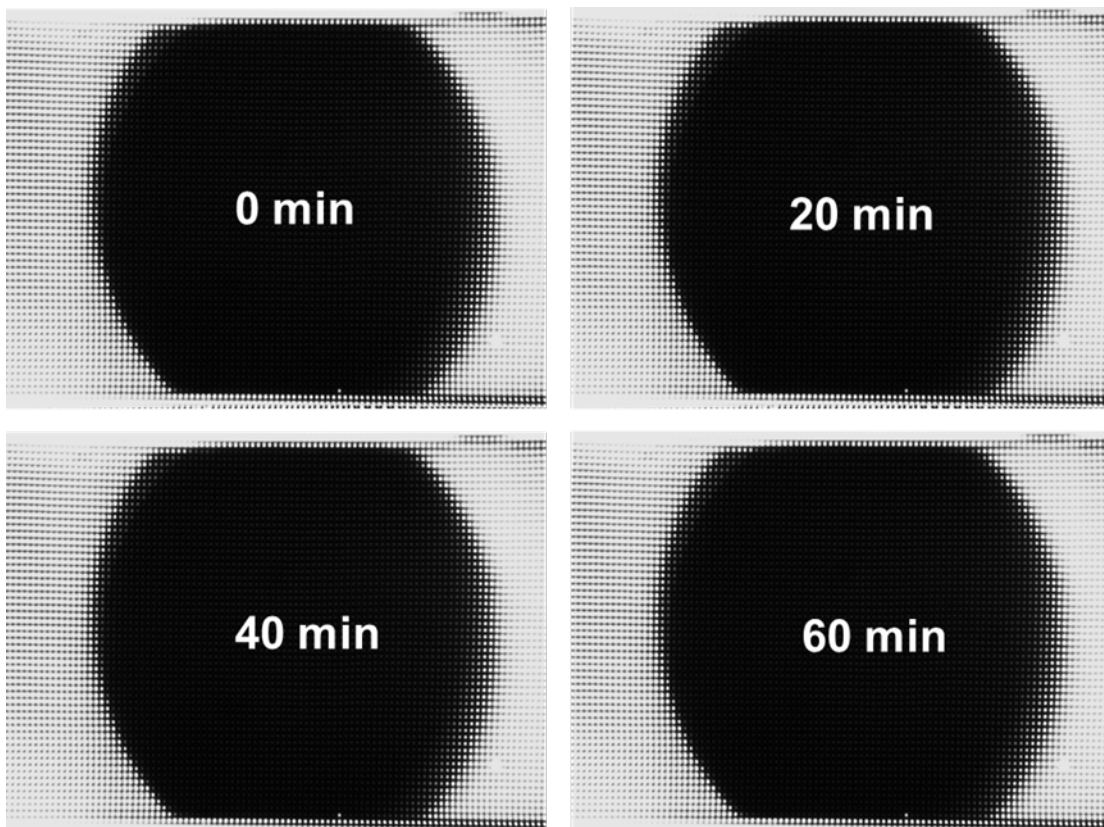


Figure S1. Characterization of sealing performance. No diffusion of fluorescent dyes into the photobleached area was observed over 60 min after sealing with the mechanical press.

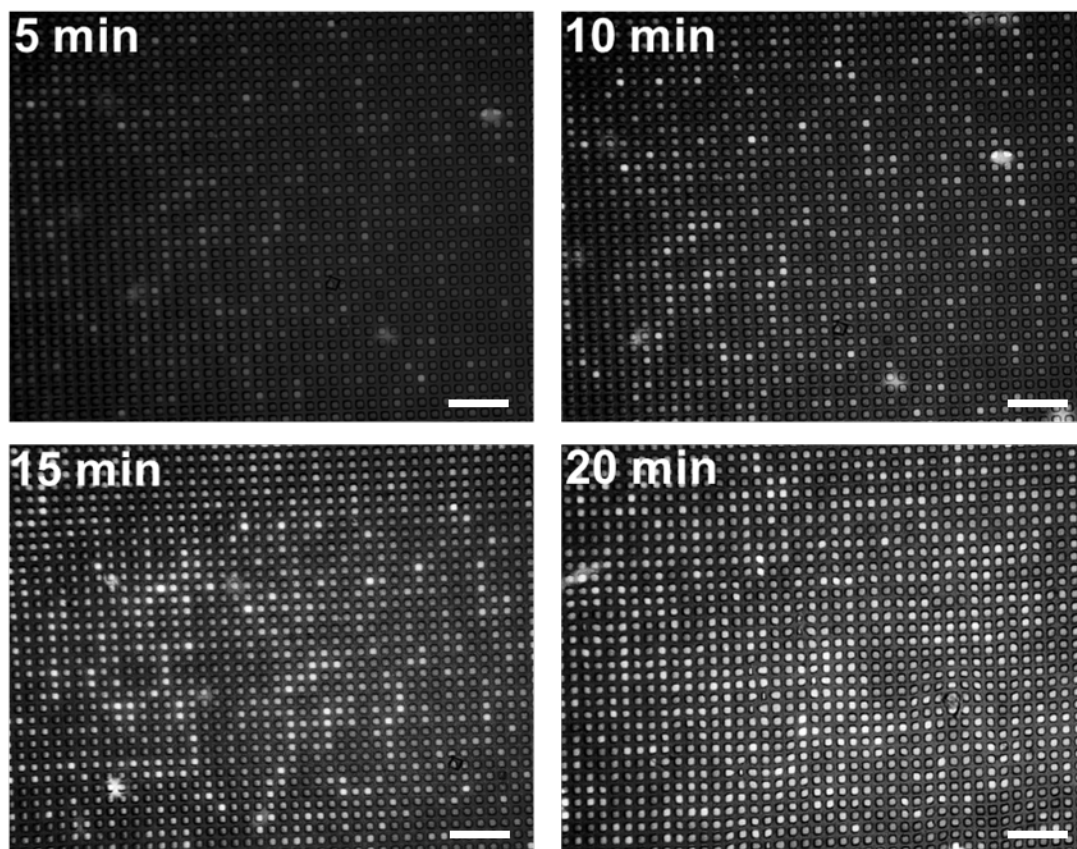


Figure S2. Representative fluorescence images for monitoring the signal intensity of individual fL reactions over 20 min (scale bar is 100 μm).

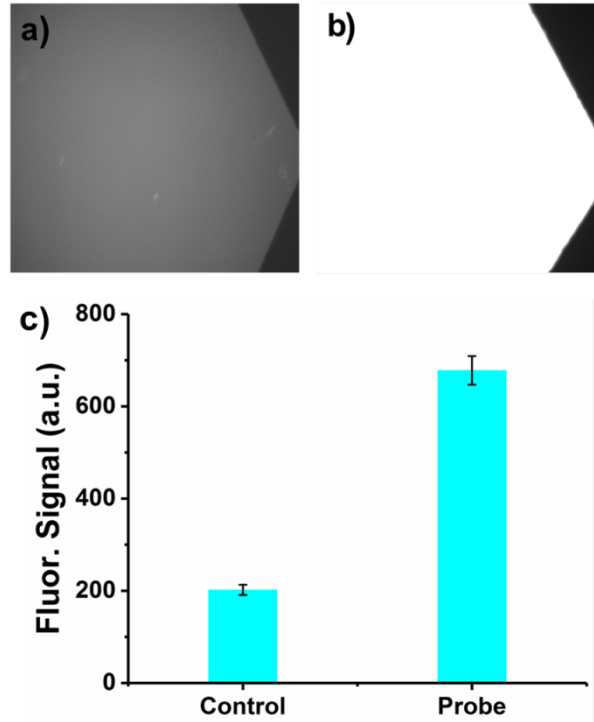


Figure S3. Fluorescent images (a) before and (b) after immobilization of 3'-FAM labelled capture probes on APTES and glutaraldehyde treated glass slide, and (c) corresponding intensity of fluorescent signals.

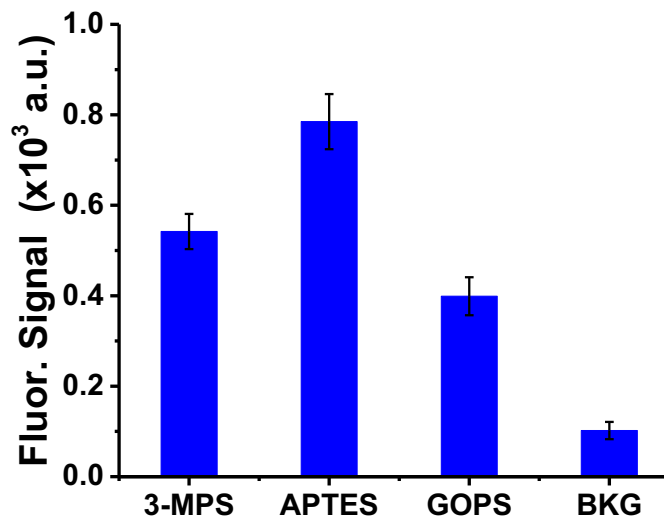


Figure S4. Optimization of surface treatment of glass substrate. The protocols of surface modification were adopted from the prior report.¹

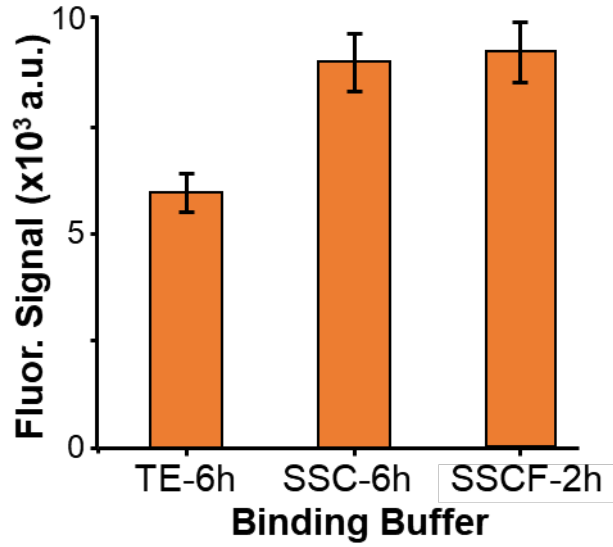


Figure S5. Optimization of the binding buffer and incubation time for the double hybridization assay.

Table S1. Probability Calculated by Poisson Distribution.

Average rate of occurrence, λ	Number of occurrences, k	Probability $P(X=k)$. %
1	0	36.8
	1	36.8
	≥ 2	26.4
0.1	0	90.5
	1	9.05
	2	0.905
0.01	0	99.0
	1	0.990

Table S2. Sequences of Capture and Detection Probes for *GAPDH* and *EWS-FLI* type 1 and type 3 Transcripts.

Probes	Oligo Sequence	Location in Fusion mRNA
<i>GAPDH</i>		
Capture probe CP1	5'-NH ₂ -C ₁₂ -AGGTCCACCACTGACACGTTG-3'	
Detection probe DP1	5'-GCAGTGGGGACACGGAAGGCC-TEG-biotin-3'	
Detection probe DP2	5'-TGTAGTTGAGGTCAATGAAGGG-TEG-biotin-3'	
<i>EWS-FLI</i> Type 1		
Capture probe CP2	5'-NH ₂ -C ₁₂ -GCACTTGCGAATCTGCTTGA-3'	FLI1, exon 9
Detection probe DP3	5'-GCAACTCTTGTCCCAGTCCTC3'-TEG-biotin-3'	EWS, exon 1
Detection probe DP4	5'-CTGGATAAGCAGGCTGAGTG3'-TEG-biotin-3'	EWS, exon 5
<i>EWS-FLI</i> Type 3		
Capture probe CP2	5'-NH ₂ -C ₁₂ -GCACTTGCGAATCTGCTTGA-3'	FLI1, exon 9
Detection probe DP5	5'-TGGGTCCACCAGGCTTATTG3'-TEG-biotin-3'	EWS, exons 9, 10
Detection probe DP6	5'-GGTGGTCCTGTCGGAATGAA3'-TEG-biotin-3'	EWS, exon 8

Table S3. Synthetic *GAPDH* Oligonucleotides Sequence.

Synthetic <i>GAPDH</i> oligonucleotides sequence
5'-CAAGGUCAUCCCUGAGCUGAACGGGAAGCUCACUGGCAUGGCCUUC CGUGUCCCCACUGCCAACGUGUCAGUGGUGGACCUGACCUGCCGUCU AGAAAAACCUGCCAAAUAUGAUGACAU-3'

Table S4. Common Types of PNET Fusion and Corresponding Genetic Breakpoints.

Fusion Type	Fusion Exons
<i>EWS-FLI1</i> type 1	<i>EWS</i> (1-7) + <i>FLI</i> (6-9)
<i>EWS-FLI1</i> type 2	<i>EWS</i> (1-7) + <i>FLI</i> (5-9)
<i>EWS-FLI1</i> type 3	<i>EWS</i> (1-10) + <i>FLI</i> (6-9)
<i>EWS-ERG</i>	<i>EWS</i> (1-7) + <i>ERG</i> (6-10)

Table S5. Characterization of EVs Isolated from CHLA-9 and CHLA-258 Cells.

Sample	Concentration (/mL)	Mean diameter (nm)
CHLA-9 EVs	1.17×10^{12}	152.1
CHLA-258 EVs	2.08×10^{11}	127.3

REFERENCES:

1. Goddard, J.; Erickson, D., *Anal. Bioanal. Chem.* **2009**, 394 (2), 469-479.